ARTICLE

The Effect of Synthesis Conditions and Humidity on Current−Voltage Relations in Electrodeposited ZnO-Based Schottky Junctions

Shawn Chatman and Kristin M. Poduska*

Department of Physics and Physical Oceanography, Memorial University of Newfoundland, St. John's, Newfoundland A1B 3X7, Canada

ABSTRACT Electrochemically produced ZnO/metal rectifying (Schottky) junctions can exhibit consistent barrier heights and high rectifying ratios when prepared using optimized electrolyte pH (6.5) and applied voltage (≤−1.1 V vs Ag/AgCl) conditions. An increase in soft breakdown for more acidic deposition electrolytes (pH 4) correlates with a diminished preferred orientation in the resulting ZnO electrodeposit. Forward-biased junctions exposed to increased relative humidities show increased current as a result of protonic conduction from water hydrolysis at the ZnO/air interface. At moderate to high relative humidities (50−85% RH), hydrophobic coatings improve the quality of the rectifying response by changing the wetting properties of the ZnO surface. Our findings suggest that electrodeposition, in conjunction with postdeposition surface coatings, can offer improved functionality for electron transport materials in wet or humid environments.

KEYWORDS: metal oxides • rectifying junctions • electrodeposition • electrical resistivity • X-ray diffraction • hydrophobic surfaces

INTRODUCTION

Ceramic semiconducting materials exhibit electrical and optical characteristics that can be utilized in a range of electronic devices, so it is of great technological importance to control electron transport to and through such materials. A prime example is ZnO, which is a well-known semiconductor (1) that shows promise in electronic device applications ranging from transparent transistors (2,3) to chemical sensors (4, 5). ZnO can manifest humidity-related changes in its electronic properties such as resistivity, rectification, and capacitance (5, 7, 8). Different mechanisms to explain the origin of humidity effects for metal oxide materials have been proposed, including temperature- or voltage-dependent chemisorption (7, 9−11). Here we show that electrochemically prepared ZnO rectifying (Schottky) junctions have current−voltage relationships that are influenced by relative humidity changes at ambient temperatures because of a water electrolysis mechanism (12, 13), and that their responses can be qualitatively changed by varying electrolyte pH during electrodeposition or by adding postdeposition coatings. These findings highlight the effect that wet or humid environments can have on electron transport materials.

The relationship between humidity and electron transport in ZnO has been investigated in diverse contexts. For example, ZnO has been widely studied as a ceramic material for humidity sensing applications (5, 8, 7, 10). When used in rectifying *pn* heterojunction humidity sensors, it has been proposed that the electrolytic decomposition of water at the junction continually refreshes the surface to prolong device operation (13). In contrast, other studies have shown that electrolysis of condensed water can contribute to undesirable degradation in ZnO-based varistors (14) that are exposed to water vapor during the course of their normal operation.

ZnO-based Schottky junctions are typically fabricated using high-temperature, high-vacuum, or sol−gel processes (7−9). Our alternative approach is to use electrochemical deposition to form the rectifying junction. Electrodeposition is a technique that has been used to make ZnO thin films (15−19), but reports of its electrical resistivity have more often been associated with its function in multilayer systems (20−23) rather than ZnO alone (24). Furthermore, none have investigated the impact of humidity changes on electrical responses in electrodeposited ZnO, despite the fact that this synthesis method offers options for controlled deposit epitaxy and porosity (17−19).

EXPERIMENTAL METHODS

ZnO Electrosynthesis. We electrodeposited thin films of ZnO by modifying (19) an existing procedure based on nitrate reduction in aqueous electrolytes (15). Yoshida et al. have reported that the formation of ZnO in this process is due to a multistep precipitation/reduction reaction at the working electrode surface (16), as shown in eqs 1and 2.

* Corresponding author. E-mail: kris@mun.ca. Phone: (709) 737-8890. Fax: (709) 737-8739.
Received for review September 11, 2008 and accepted November 18, 2008
DOI: 10.1021/am800049u

Published on Web 02/20/2009

$$NO_3^- + H_2O + 2e^- \rightarrow NO_2^- + 2OH^- \quad (1)$$

$$Zn^{2+} + 2OH^- \rightarrow Zn(OH)_2 \rightarrow ZnO + H_2O \quad (2)$$

Zn^{2+} ions adsorbed on the working electrode surface facilitate the reduction of nitrate to nitrite, producing excess hydroxide ions and increasing the local pH. This pH increase allows the formation of $Zn(OH)_2$ on the surface of the working electrode, which spontaneously decomposes to ZnO at temperatures above 50 °C (16, 18).

Previous work from our group addressed the synthesis conditions required for ZnO electrodeposits displaying either ohmic or rectifying contacts with the underlying conducting metal substrates (24). In the present work, we identify an expanded range of deposition conditions that can be used to synthesize rectifying ZnO contacts, with dramatically improved performance, by adjusting electrolyte pH. Samples were deposited at potentials ranging from −2.0 to −0.7 V vs. an Ag/AgCl reference, from an electrolyte of 0.01 M $Zn(NO_3)_2$ (ACS reagent grade, SCP Science) in ultrapure water (18.2 MΩ cm, Barnstead Nanopure), using NaOH or HCl to adjust the pH between 4.0 and 7.0. Mechanically polished stainless steel (316 series) substrates were cleaned by ultrasonication prior to use.

Characterization. X-ray diffraction (XRD) data were collected with a Debye−Scherrer powder diffractometer (Rigaku D/MAX 2200PC) using Cu*K*α radiation in the $\theta-\theta$ geometry. Scan parameters were typically 20−80° 2θ, at a rate of 6°/min with a step size of 0.03° 2θ. Diffuse reflectance spectroscopy (Ocean Optics USB2000, data not shown) confirmed that all electrodeposited samples showed well-defined optical absorption edges corresponding to bandgap energies consistent with ZnO (3.2−3.3 eV) (1). Scanning electron microscopy (FEI Quanta 400) provided cross-sectional views of the electrodeposits to assess thickness uniformity, and qualitative elemental composition comparisons among different samples were made with a dispersive X-ray (EDX) analytical system (Roëntec). Electrodeposit and postdeposition overcoat thicknesses were measured with an atomic force microscope (Asylum Research MFP-3D).

Electrical Properties. The current−voltage (*I*−*V*) characteristics of electrodeposits were collected with either a Hokuto Denko HA 501 potentiostat or a Keithley 2100 Sourcemeter under varying humidity conditions. Relative humidity was controlled using a sealable plastic cell with adjustable vents. Dessicant and water vapor were used to adjust the relative humidity of the cell between 15 and 85% (±7%). All DC data were were collected and analyzed with LabVIEW (National Instruments, customized in-house). Electrical connections to the samples involved low-resistance (<1 Ω) ohmic stainless steel or aluminum compression contacts. Contact areas (∼ 4 mm^2) were large compared to individual crystallite sizes (typically 100−1000 nm in diameter), so we assume that all electrical measurements involved conduction through and/or across many ZnO grains.

RESULTS AND DISCUSSION

Electrodeposit Characterization. XRD data from electrodeposits (Figure 1) were compared with standard diffraction data for hexagonal ZnO (JCPDS 36−1451) and zinc metal (JCPDS 04−0831) (25). All observed peaks can be indexed to either ZnO or the substrate. However, the presence or absence of Zn metal is difficult to confirm definitively from XRD data because two of the strongest Zn Bragg reflections would appear near (and overlap with) the ZnO (101) and substrate peaks.

Although the electrodeposits appear to be phase-pure based on XRD data, investigations of the ZnO/substrate interface suggest that compositional differences do exist. To facilitate SEM and EDX investigations, we coated the substrate-supported electrodeposits with epoxy and then immersed them in liquid nitrogen to separate the ZnO from the steel substrate, allowing for comparative analysis at both the ZnO/air and the ZnO/substrate interfaces. Differences in the contrast of backscattered electron images from the two ZnO interfaces, in conjunction with elemental composition information from complementary EDX measurements, suggest that there is a higher Zn content at the ZnO/substrate interface. We note that high Zn content at this interface coincides with rectifying current−voltage responses, described in more detail elsewhere (24).

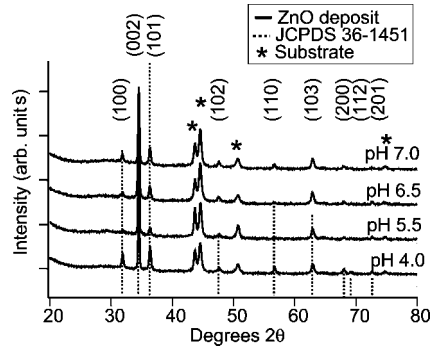

FIGURE 1. Representative indexed XRD patterns from thin films (1.0 ± 0.2 μm thickness) of ZnO prepared by deposition from electrolytes with different bulk pH values. Lattice constant refinements of the indexed peaks yield excellent agreement with ZnO (JCPDS #36−1451) (25). Bragg peaks due to the stainless steel substrates are marked with an asterisk (*).

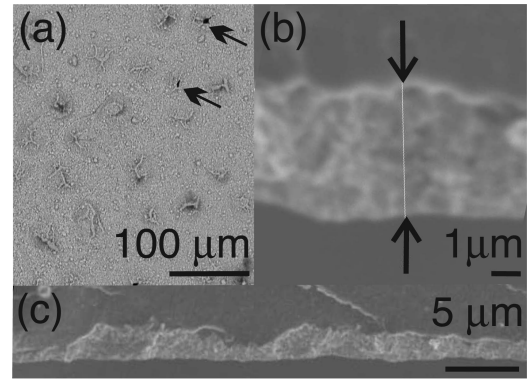

FIGURE 2. Representative SEM images showing (a) the top (air interface) of a ZnO electrodeposit, and (b,c) cross-sectional views. This deposit was prepared from an electrolyte with bulk pH 5.5 at −1.1 V. The arrows in the top view in (a) show that occasional pinholes in the film exist. The cross-sectional view in (b) highlights the polycrystalline grains in the electrodeposit, whereas (c) shows typical thickness changes across the deposit.

Cross-sectional SEM images (Figure 2b,c) emphasize that electrodeposits are polycrystalline films whose thicknesses vary across the sample (typically 1−3 μm). These films are generally continuous, but occasional holes are visible, such as those denoted with arrows in Figure 2a.

Effects of Synthesis Conditions on Rectifying Behavior. The rectifying function of an ideal Schottky junction is based on the relative Fermi energy levels between an *n*-type semiconductor and metal (26), as shown schematically in Figure 3. If, when isolated, the Fermi energy of

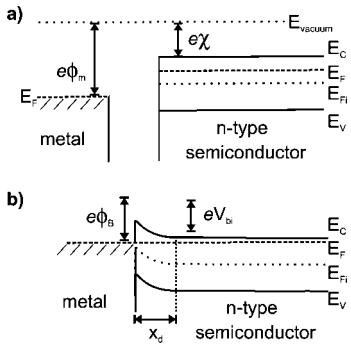

FIGURE 3. Schematic energy band diagram for (a) isolated metal and *n*-type semiconductor and (b) a Schottky junction. The work function of the metal (ϕ_m) and the electron affinity of the semiconductor (χ) are given relative to vacuum level (E_{vacuum}). In the *n*-type semiconductor, the Fermi energy (E_F) is closer to the conduction band energy (E_C) than the valence band energy (E_V). The intrinsic Fermi energy (E_{Fi}) is located midway between E_C and E_V. (b) Once the metal and semiconductor come into contact, a Schottky barrier (ϕ_B) forms at the interface and the semiconductor bands bend by an amount V_{bi} over the distance x_D.

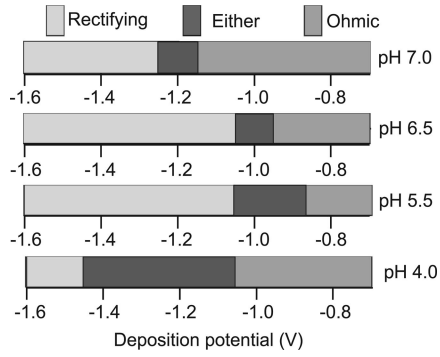

FIGURE 4. Deposition potential ranges for forming ohmic or rectifying ZnO/metal junctions depend on electrolyte pH. In all cases, there is a range of voltages for which there is poor selectivity between Schottky and ohmic responses.

the semiconductor is higher than that of the metal, then electrons in the semiconductor will move to the lower energy states in the metal to equilibrate the Fermi energies, once contact is established. As a consequence, electrons in the semiconductor encounter a potential barrier, V_{bi}, that limits flow into the metal. This barrier can be reduced by applying a positive voltage to the metal to enable thermally excited electrons to flow, creating a forward bias current. Conversely, the barrier height can be increased by applying a negative bias voltage to the metal substrate. Ideally, as the negative bias increases, conduction through the junction will approach a limiting saturation current. In practice, however, very high voltages will cause a reduction in the barrier height leading to non-negligible tunneling current in the reverse direction (soft breakdown).

We analyzed the rectifying responses of electrodeposited ZnO/metal junctions that were prepared at different bulk electrolyte pH values and deposition potentials, summarized in 4. Our experiments encompassed the viable pH range for the ZnO electroprecipitation reaction: for pH values $\geq$7, spontaneous precipitation of $Zn(OH)_2$ interferes with ZnO formation (18), whereas pH values $\leq$3.5 yield substantial Zn metal deposition that degrades the integrity of the semiconducting pathway through the sample. Figure 4 shows that

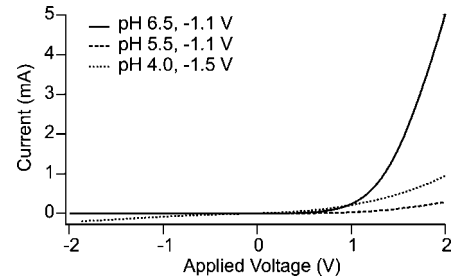

FIGURE 5. Representative *I*−*V* sweeps on electrodeposited ZnO Schottky junctions show stronger rectification and less soft breakdown with an increase in deposition electrolyte pH from 4.0 to 6.5. A representative *I*−*V* curve for pH 7.0 would coincide with the data for pH 6.5, so it is omitted for clarity.

ohmic ZnO/substrate contacts form at more positive deposition potentials (with resistances of 1−10 Ω), whereas rectification occurs in samples prepared at more negative deposition potentials (with resistances of 1×10^5 to 1×10^6 Ω), consistent with earlier findings (24). There is also an intermediate range of deposition potentials for which either ohmic response or poor rectification (with pronounced soft breakdown) can result; in other words, there is poor selectivity between linear and rectifying behaviors for these deposition potentials. Nevertheless, the current−voltage response of any single sample is repeatable and does not change over time. A comparison of representative rectifying responses for samples prepared from electrolytes with different *p*H values is shown in Figure 5.

There are several factors that likely contribute to the inferior quality of the rectifying responses at the intermediate deposition potentials; all are linked to conditions that can perturb the formation of the Zn-rich ZnO/substrate interface that causes the rectifying junction behavior. First, a more acidic bulk electrolyte pH will shift the Nernst potentials of the nitrate reduction (eq 1) and hydrogen evolution reactions to more positive values. Assuming a fixed deposition potential, these Nernst potential changes lead to an increased rate of OH^- production near the working electrode surface, and these more alkaline conditions would promote ZnO formation. However, acidic electrolytes also promote metal formation, independent of these Nernst potential changes. The competition between these two factors (localized pH increase to favor ZnO formation, and acidic bulk pH to favor Zn metal formation) at the initial stages of electrodeposit formation could lead to differences in the Zn content at the ZnO/substrate interface among different samples. SEM and EDX investigations show that these compositional changes appear to be confined to within 50 nm of the ZnO/substrate interface, which corresponds to a very small fraction of the overall electrodeposit (thicknesses $\approx$ 2 μm). Thus, XRD measurements that probe the entire sample would not be expected to show evidence of significant Zn content, consistent with Figure 1.

For a more quantitative comparison, pH-dependent rectification data (like those shown in Figure 5) were fit to the Schottky relation given in eq 3.

$$J = A^{*}T^{2}\exp\left(\frac{-e\Phi_{B}}{kT}\right)\exp\left(\frac{e(V-IR)}{nkT}\right) \quad (3)$$

This expression describes the idealized exponential increase in forward current with increasing forward bias voltage (27−29), where J is current density, e is the electron charge, I is current, k is Boltzmann's constant, V is voltage, R is the series resistance, T is temperature, n is the ideality factor, and A^{*} is Richardson's constant (32 A/(cm^2 K^2)). Table 1 provides a summary of Schottky barrier heights and ideality values determined by fitting collected data to eq 3. Also included are rectifying ratios, which give the relative magnitudes of the forward bias (+2 V) and reverse bias (−2 V) currents.

A linearized form of the Schottky equation has also been used by others to extract the ideality and Schottky barrier from the linear portion of the $I-V$ curve before significant forward current flows (30)

$$\ln(J) = \frac{e}{nkT}(V-IR) - \frac{e\Phi_{B}}{nkT} + \ln(A^{*}T^{2}) \quad (4)$$

For our samples, the linearized Schottky analysis technique provided data consistent with the ideal Schottky equation but with larger uncertainties, in part due to fitting fewer data points. Therefore, only data fit to the ideal Schottky equation are included in Table 1.

Rectifying ratios show a dramatic increase for junctions prepared in less acidic deposition electrolytes (Figure 5). Regardless of electrolyte pH, Schottky barrier heights for our electrodeposited ZnO junctions compare well with values for junctions synthesized by other methods (27−29, 31). Ideality (n) values for all electrodeposited Schottky junctions are greater than 2, indicating multiple conduction pathways (31, 32).

It is not entirely clear why the more acidic electrolytes yield samples with more soft breakdown and correspondingly lower rectifying ratios. Scrutinizing the XRD data for pH-dependent differences in preferred orientation (from peak height comparisons) or particle size (from peak broadening) did not yield an obvious correlation across the entire range of pH values studied, nor do optical absorption edge data offer additional insights. However, we did observe that deposits prepared at the most acidic pH values (4.0) showed a substantial decrease in the (002) orientation that is widely observed in ZnO electrodeposits (16−19). We also observe that rectifying junctions prepared from the most acidic electrolytes have the lowest resistances (∼1 Ω at pH 4 compared to ∼1 × 10^5 Ω at pH 6.5).

Table 1. Data Obtained from Fitting Rectifying Current-Voltage Responses in Samples Prepared from Electrolytes with Different pH Values to the Ideal Schottky Equation; The Highest Rectifying Ratios Occur in Junctions Prepared from Electrolytes near Neutral pH

pH	n	Φ_{B0}	rectifying ratio
4.0	15 ± 5	0.80 ± 0.04	6 ± 4
5.5	13 ± 5	0.73 ± 0.05	100 ± 20
6.5	13 ± 5	0.85 ± 0.03	1000 ± 200
7.0	13 ± 5	0.85 ± 0.03	1000 ± 200

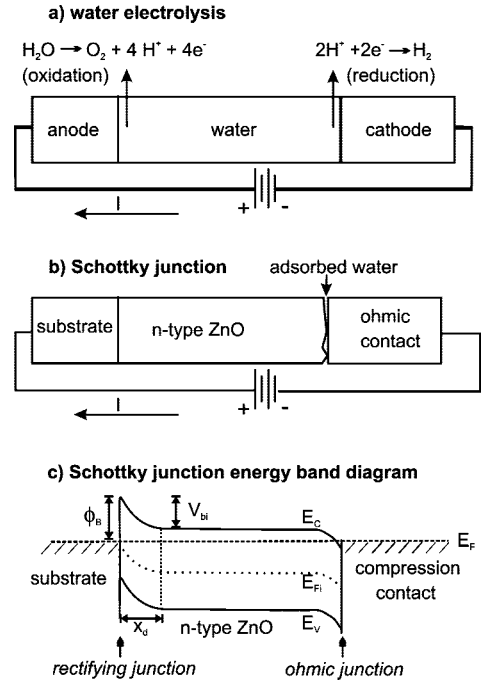

FIGURE 6. Schematic diagrams illustrate (a) the water electrolysis reaction that can occur between two metal electrodes, and (b) where the water electrolysis reaction occurs in the electrodeposited Schottky junctions (in the water adsorbed at the ZnO/air interface). The corresponding junction energy band diagram (c) emphasizes that the rectifying junction occurs at the ZnO/substrate, whereas an ohmic contact exists between the ZnO/air interface and the metal compression contact.

On the basis of these investigations of junction performance as a function of electrodeposition conditions, we conclude that deposits prepared from pH 6.5 electrolytes show the best diode functionality without the risk of spontaneous $Zn(OH)_2$ precipitation. Thus, all subsequent data are presented for electrodeposits prepared from electrolytes with this pH using a deposition potential of −1.1 V.

Humidity Effects on Rectification. Previous studies have indicated that ZnO/CuO based rectifying *pn* junctions, which are operationally similar to Schottky junctions, are sensitive to changes in relative humidity when forward biased (13). The humidity-dependent responses of this and similar systems (7, 11) has been attributed to water electrolysis at the positive and negative sides of the junction. A schematic diagram of the water electrolysis reaction, given in Figure 6a, depicts the oxidation and reduction reactions that occur at the anode and cathode, respectively. For comparison, Figure 6b shows that water vapor can adsorb to the ZnO/air interface, and this water can be electrolyzed when the ohmic compression contact acts as a cathode, whereas the ZnO acts as an anode (foward bias condition).

$$\text{(at ZnO)} \quad 2H_2O \rightleftharpoons O_2 + 4H^{+} + 4e^{-} \quad (5)$$

$$\text{(at metal)} \quad 2H^{+} + 2e^{-} \rightleftharpoons H_2 \quad (6)$$

The protons generated at the anode diffuse and can be reduced to hydrogen by electrons at the cathode surface. Combining current responses due to the ideal Schottky junction conduction (eq 3) with the electrolysis-generated

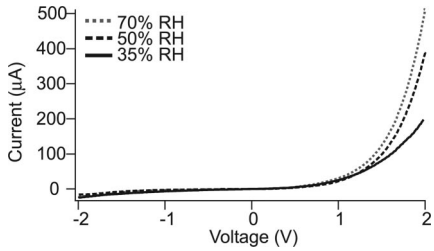

FIGURE 7. *I*−*V* sweeps on electrodeposited Schottky junctions show larger forward bias currents at higher relative humidities.

proton conduction yields a total current density expression with three components

$$J = A^{*}T^{2}\exp\left(\frac{-e\Phi_{B}}{kT}\right)\exp\left(\frac{e(V-IR)}{nkT}\right) + Ck_{f}[H_{2}O]^{\frac{1}{2}}[H^{+}] - Ck_{r}[O_{2}]^{\frac{1}{4}}[H^{+}] \quad (7)$$

where C is a constant and k_f and k_r are the forward and reverse reaction rates from eqs 5 and 6. The second term in eq 7 is due to the physisorbed water electrolysis and increases with both humidity and voltage increases. The third term counteracts the forward bias current and is due to the oxygen partial pressure of the system (13). The rectifying behavior of the Schottky contact ensures that there is little reverse bias current, even in the presence of water electrolysis. We note that relative magnitudes of the protonic conduction, based on electrolysis and charge movement through adsorbed water, and the Schottky (thermionic emission) current are dependent on applied bias voltage. In our samples, the current resulting from the electrolysis-generated proton conduction (∼10 mA) greatly outweighs the contribution of the Schottky current (∼10−100 μA). Because of the polycrystalline nature of our samples, grain boundary contributions dominate the electrical resistance of our samples relative to the thickness-dependent resistance of the ZnO itself. This fact, in conjunction with the surface-based water electrolysis mechanism, implies that the details of the ZnO/air interface are more important for the magnitude of the forward current flow (which can vary by an order of magnitude, from 100 to 1000 μA) than film thickness (with smaller percentage uncertainties of 1.0 ± 0.2 μm).

Figure 7 illustrates the role that humidity plays in the quality of the rectifying response in electrodeposited ZnO Schottky junctions. For low humidities (≤50%), Schottky junctions show *I*−*V* sweeps with minimal signs of soft breakdown at reverse bias and good rectifying ratios (∼1000). However, higher relative humidities lead to noticeable signs of soft breakdown at reverse bias, as well as increased noise at forward bias. At the highest humidities (>70%), the forward current can also show erratic responses, in both direction and magnitude, to humidity changes. Nevertheless, the ZnO electrodeposits display excellent adherence to the substrate, even with repeated cycling to high (75−95%) relative humidities. There were no other visible signs of sample degradation, such as color changes (14), upon repeated exposure to high relative humidities and bias voltages.

Although these electrodeposited junctions do exhibit humidity-sensitive *I*−*V* responses under sweeping voltage conditions for constant relative humidities, they do not function effectively as traditional humidity sensors that operate at a fixed bias voltage in changing relative humidity environments. For example, although abrupt current changes are observed in junctions forward biased at 1−2 V when exposed to intervals of alternating 50 and 80% relative humidities, there is also substantial drift in the current in between these humidity changes. Thus, it is not possible to calibrate the junction so that a specific current indicates a specific relative humidity value. Additional details, including a representative plot of current *vs*. time for junctions exposed to different relative humidities, is provided as Supporting Information.

For completeness, we note that ohmic electrodeposited ZnO/substrate junctions are also affected by humidity, but the effects are much less pronounced. The humidity-dependent increase in resistance is ≤1% (1−5 Ω) for ohmic samples cycled between 15 and 80% relative humidity. In the context of the water electrolysis mechanism described above, proton conduction (∼10 mA) is negligible compared to the larger currents that can flow through the lower-resistance ohmic samples (400−600 mA at 2 V), leading to a much weaker humidity-related effects.

Surface Coating Effects on Rectification. Because erratic current responses in our junctions are more prevalent at high relative humidities, it is possible that this problem is due to a dynamic contact area between the ZnO and metal pressure contact as more water vapor adsorbs and begins to condense at the junction for the highest humidity levels. (This effect could be separate from the water electrolysis-based degradation that has been observed in other ZnO-based devices (14).) To this end, we investigated the effect of thin surface coatings, applied postelectrodeposition, at the ZnO/air interface.

Hydrophobic coatings and materials have been widely studied recently, but there has been little focus on the role that hydrophobicity can play in controlling the electronic response of ceramic rectifying junctions. Some reports have used hydrophobic coatings to preserve the integrity of humidity sensitive polymers (33, 34). Our results suggest that this is an avenue worth investigating to control the quality of the rectifying response in junctions that may be adversely affected by changes in relative humidity.

We find that adding a hydrophobic coating, to change the way that water adsorbs and condenses the ZnO/air interface, can lead to improved rectifying responses of our junctions. Best results were obtained by applying a thin layer of aliphatic petroleum distillates (Stoddard solvent, mean molecular weight 144 g/mol, dissolved in a 1:10:10 mixture of xylene, propane and butane, Kiwi Outdoor Camp Spray). These layers accentuate the natural hydrophobicity of our ZnO electrodeposits. (This hydrophobicity, consistent with other reports (35), is in part due to the surface roughness of the electrodeposits (19, 24).) Assessments of coating continuity and thickness using AFM showed that the hydrophobic layers appear continuous on length scales greater than ∼100 nm and typically vary in thickness from 10 to 60 nm. Pooling

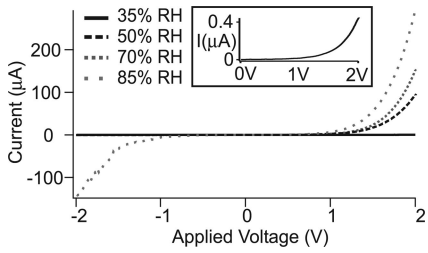

FIGURE 8. Sprayed hydrophobic coatings reduce soft breakdown, except at the highest relative humidity values (≥85%). The inset shows the same data with a smaller current scale to emphasize the rectifying nature of the *I*−*V* response at 35% RH.

of the coating mixture does occur in deep features of the deposit, leading to substantially thicker coatings in some places.

Figure 8 shows that electrodeposits with these coatings exhibit less soft breakdown at high relative humidities (50−70%), and rectifying ratios that are comparable to those observed at lower humidities. At the highest relative humidities (≥85%), it is still possible to observe erratic changes in current, but the magnitude of the changes are much smaller than for uncoated junctions.

The continuity and thickness of the hydrophobic coating can impact how effectively it suppresses soft breakdown in the junctions at higher relative humidities. For example, thin layers of silicone (applied in a manner similar to the petroleum distillates) did not coat the junctions as uniformly, leaving some exposed regions. The corresponding Schottky responses showed somewhat improved rectification over uncoated samples, but more soft breakdown occurred relative to the data shown in Figure 8. In other experiments, more complete electrically insulating coatings were applied by submersing junctions in a solution of 5 mM octadecyltrichlorosilane (OTS) in toluene while confined to a desiccated glovebox, following a method reported earlier (35). This procedure yielded coatings whose continuity and thickness were comparable to the sprayed coatings, according to AFM investigations. However, through-sample resistances were prohibitively high (0.5−50 MΩ) and unstable, suggesting that the coatings acted as electrical insulation between the ZnO and metal compression contacts. For all silicone and OTS-coated samples, removal of the coatings with ethanol or acetone restored the original rectifying behavior. The current vs time trends during exposure to different relative humidities for representative coated and uncoated junctions is provided as Supporting Information.

For comparison, we also addressed the effect of metallic coatings that still preserve enough surface roughness to allow the samples to remain hydrophobic. Aluminum (65 ± 15 nm or 200 ± 30 nm thicknesses) were thermally evaporated at 1×10^{-3} torr onto rectifying ZnO deposits. After coating, sample resistances fell from $\sim 1 \times 10^{6}$ Ω to ~1 Ω, eliminating the rectifying responses. Although cross-section SEM shows that our films are largely continuous, these resistance measurements suggest that aluminum may permeate pinholes in the film (Figure 2a), bypassing the conduction pathway through the bulk ZnO and effectively short-circuiting the Schottky junction. Aluminum could also be in contact with the ZnO depletion layer, which would adversely affect the desired Schottky band bending at the ZnO/metal substrate interface.

CONCLUSIONS

The quality of the rectifying responses in electrodeposited ZnO/metal junctions, including the magnitude of currents during forward bias and soft breakdown effects during reverse bias, can be optimized by adjusting the deposition potential and the bulk electrolyte pH. These two parameters can be used to control the propensity to form the Zn-rich interface (during the initial stages of film growth) that causes the rectifying behavior. Additionally, hydrophobic coatings at the ZnO/air interface can further decrease soft breakdown and improve the rectifying ratios at moderate relative humidities, if the coatings are both continuous and do not electrically insulate the ZnO from the ohmic compression contact. We expect that this use of postdeposition surface coatings could be relevant for other inorganic materials and devices whose electronic operation is degraded in humid or wet environments.

Acknowledgment. We thank H. Gillespie (XRD) and M. Schaffer (SEM/EDX) for use of instrument facilities at the Memorial University of Newfoundland and L. Emberley for assistance with sample preparation. We also acknowledge financial support from the Natural Science and Engineering Resource Council (Canada), Canada Foundation for Innovation New Opportunities Fund, and Memorial University of Newfoundland.

Supporting Information Available: Current vs time trends during exposure to different relative humidities for representative coated and uncoated Schottky junctions. This material is available free of charge via the Internet at http://pubs.acs.org.

REFERENCES AND NOTES

(1) Özgür, Ü.; Alivov, Y. I.; Liu, C; Teke, A.; Reshchikov, M.A.Dõ; gan, S.; Avrutin, V.; Cho, S.-J.; Morkoç, H *J. Appl. Phys.* **2005**, *98*, 041301/1−103.
(2) Fortunato, E.; Barquinha, P.; Pimentel, A.; Gonçalves, A.; Marques, A.; Pereira, L.; Martins, R. *Thin Solid Films* **2005**, *487*, 205–211.
(3) Wager, J. F. *Science* **2003**, *300*, 1245–1246.
(4) Schmidt-Mende, L.; MacManus-Driscoll, J. L. *Mater. Today* **2007**, *10*, 40–48.
(5) Barsan, N.; Koziej, D.; Weimar, U. *Sens. Actuators, B* **2007**, *121*, 18–35.
(6) Batzill, M.; Diebold, U. *Phys. Chem. Chem. Phys.* **2007**, *9*, 2307–2318.
(7) Chen, Z.; Lu, C. *Sensor Lett.* **2005**, *3*, 274–295.
(8) Lee, C.-Y.; Lee, G.-B. *Sensor Lett.* **2005**, *3*, 1–15.
(9) Fenner, R.; Zdankiewicz, E. *IEEE Sensors J.* **2001**, *1*, 309–317.
(10) Traversa, E.; Bearzotti, A. *Sens. Actuators, B* **1995**, *23*, 181–186.
(11) Kulwicki, B. M. *J. Am. Ceram. Soc.* **1991**, *74*, 697–708.
(12) Chakrapani, V.; Angus, J. C.; Anderson, A. B.; Wolter, S. D.; Stoner, B. R.; Sumanasekera, G. U. *Science* **2007**, *318*, 1424–1430.
(13) Yoo, D. J.; Park, S. J. *J. Electrochem. Soc.* **1996**, *143*, L89−L91.
(14) Chen, W.-P.; Chan, H. L. W. *J. Am. Ceram. Soc.* **2002**, *85*, 1625–1627.
(15) Izaki, M.; Omi, T. *Appl. Phys. Lett.* **1996**, *68*, 2439–2440.
(16) Yoshida, T.; Komatsu, D.; Shimokawa, N.; Minoura, H *Thin Solid Films* **2004**, *451−452*, 166–169.
(17) Lincot, D. *Thin Solid Films* **2005**, *487*, 40–48.
(18) Limmer, S. J.; Kulp, E. A.; Switzer, J. A. *Langmuir* **2006**, *22*, 10535–10539.

(19) Ren, T.; Baker, H. R.; Poduska, K. M. *Thin Solid Films* **2007**, *515*, 7976–7983.
(20) Zhang, D. K.; Liu, Y. C.; Liu, Y. L.; Yang, H. *Physica B* **2004**, *351*, 178–183.
(21) Katayama, J.; Ito, K.; Matsuoka, M.; Tamaki, J. *J. Appl. Electrochem.* **2004**, *34*, 687–692.
(22) Mondal, A.; Mukherjee, N.; Bhar, S. K. *Mater. Lett.* **2006**, *60*, 1748–1752.
(23) Izaki, M.; Shinagawa, T.; Mizuno, K.-T.; Ida, Y.; Inaba, M.; Tasaka, A. *J. Phys. D: Appl. Phys.* **2007**, *40*, 3326–3329.
(24) Chatman, S.; Ryan, B. J.; Poduska, K. M *Appl. Phys. Lett.* **2008**, *92*, 012103/1−3.
(25) Powder Diffraction File; Joint Commission on Powder Diffraction Standards, International Centre for Diffraction Data: Newtown Square, PA, 2003; www.icdd.com.
(26) Wager, J. F. *Thin Solid Films* **2008**, *516*, 1755–1764.
(27) Oh, M.-S.; Hwang, D.-K.; Lim, J.-H.; Choi, Y.-S.; Park, S.-J *Appl. Phys. Lett.* **2007**, *91*, 042109/1−3.
(28) Kim, S.-H.; Kim, H.-K.; Seong, T.-Y *Appl. Phys. Lett.* **2005**, *86*, 112101/1−3.
(29) Liang, S.; Sheng, H.; Liu, Y.; Huo, Z.; Lu, Y.; Shen, H. *J. Cryst. Growth* **2001**, *225*, 110–113.
(30) Gupta, R. K.; Singh, R. A. *Mater. Sci. Semicond. Process.* **2004**, *7*, 83–87.
(31) Brillson, L. J.; Mosbacker, H. L.; Hetzer, M. J.; Strzhemechny, Y.; Jessen, G. H.; Look, D. C.; Cantwell, G.; Zhang, J.; Song, J. J *Appl. Phys. Lett.* **2007**, *90*, 102116/1−3.
(32) Newton, M. C.; Firth, S.; Warburton, P. A *Appl. Phys. Lett.* **2006**, *89*, 072104/1−3.
(33) Lv, X.; Li, Y.; Hong, L.; Luo, D.; Yang, M. *Sens. Actuators, B* **2007**, *124*, 347–351.
(34) Ueda, M.; Nakamura, K.; Tanaka, K.; Kita, H.; Okamoto, K. *Sens. Actuators, B* **2007**, *127*, 463–470.
(35) Badre, C.; Pauporté, T.; Turmine, M.; Dubot, P.; Lincot, D. *Physica E* **2008**, *40*, 2454–2456.

AM800049U